Modeling and Control of Hybrid Electric Vehicles: A Case Study for Agricultural Tractors

Chao Jia, Wei Qiao, and Liyan Qu
Power and Energy Systems Laboratory
Department of Electrical and Computer Engineering
University of Nebraska-Lincoln
Lincoln, NE, 68588-0511 USA
cjia@huskers.unl.edu; wqiao3@unl.edu; lqu2@unl.edu

***Abstract*—To reduce fuel consumption and pollutant emissions, there is an increasing interest in electrification of non-road mobile machinery such as agricultural tractors (ATs). This paper presents a high-fidelity forward model for series hybrid electric agricultural tractors (HEATs). To tackle the control problem caused by the mixed power loads and complicated tractor-implement operations, two benchmarking rule-based power management strategies, thermostat (TC) and power follower control (PFC), are designed and investigated. Based on the typical working cycles, the simulation results show PFC realizes better performance in saving fuels and reducing nitrogen oxides (NOx) and carbon monoxide (CO) emissions at the cost of producing more particulate matter (PM).**

Keywords—agricultural tractor (AT), emissions, fuel economy, power management strategy (PMS), rule-based control, series hybrid electric vehicle (HEV).

I. INTRODUCTION

Non-road mobile machinery (NRMM) is mainly used in agricultural and construction applications and powered by diesel engines. The NRMM is a considerable source of air pollution emissions and fuel consumption in the United States and the European Union [1]. The increasingly stringent regulations and standards have not only spurred the development in the engine design and after-treatment technologies, but also accelerated the technology transfer from on-road to non-road machinery [2]. In the automotive industry, the electrification of light-duty and on-road heavy-duty vehicles has been proved to be one of the most viable strategies to reduce emissions and energy consumption. Likewise, there is an increasing interest in the electrification of heavy off-road machinery, such as agricultural tractors (ATs), to achieve the same goals without compromising their functionality and performance [3]. Besides, the electrification of ATs also offers significant benefits in terms of controllability and reliability, which can enable operators to save both time and money.

The areas of ATs' electrification can be divided into four categories: engine auxiliaries, electric traction drives, energy storage, and implement electrification [4]. Similar to the on-road hybrid electric vehicles (HEVs), several commonly used on-board energy storage systems such as batteries, ultracapacitors, and flywheels can be utilized for hybrid electric agricultural tractors (HEATs).

This work was supported in part by the Nebraska Public Power District (NPPD) through the Nebraska Center for Energy Sciences Research (NCESR).

Researchers have investigated various powertrain configurations of HEATs. For the micro and mild hybridization, the parallel architecture is preferable. However, since more and more electric power is required in the tractor-implement electrification system, a dedicated generator is of paramount importance [2]. The series configuration takes advantage of decoupling loads and drives from the engine and, therefore, allows the engine to run at the maximum efficiency and in the lower emission region under varying load conditions. Since there is no mechanical connection between the engine and the wheels, this architecture is rather flexible with regard to the location of the powertrain components. Therefore, the series configuration is adopted in this work.

The key idea of the power management strategy (PMS) in series HEVs is to operate the engine efficiently while maintaining the battery SOC within acceptable limits. One of the main categories of the PMS is rule-based control such as thermostat control (TC), power follower control (PFC) [5], and fuzzy logic control [6]. This category of the PMS is designed based on human expertise, heuristic, or even a mathematical model without a *priori* knowledge of a predefined driving cycle [7]. Although the TC and PFC have been proposed for almost two decades, they are still popular in series-type HEVs. They have been successfully applied in commercial HEVs owing to the merits of simple implementation for real-time applications and good robustness against uncertainty. In recent years, some modified PMSs, such as hybrid thermostat strategy [8], exclusive operation strategy [9], and modified TC and PFC for three energy sources [10], were investigated to achieve better performance. Moreover, the conventional TC and PFC have been commonly used as the benchmark to evaluate a new PMS [8]-[12].

The difficulty of power management for HEATs lies in the specific traits on their operations. Unlike most on-road vehicles, ATs not only need to propel themselves but also have to provide traction force and mechanical, hydraulic, and/or electrical power for agricultural implements to perform their intended functions [13]. Therefore, the PMS of a HEAT is required to simultaneously handle mixed power demands such as PTO power, drag loading, and hydraulic loading. Furthermore, the driving and load patterns of ATs are much more complicated than those of on-road vehicles. In general, an AT can be used for transport and a variety of field operations

978-1-5386-6203-8/18/$31.00 ©2018 IEEE

such as harrows, swathing, balers, front loaders, and manure spreaders. The distribution of the operating points for these field operations is clearly different [14]. The former two issues have not been well addressed in the area of power management for series HEATs.

In the literature, simplified and idealized backward models are commonly used for simulation and validation of PMSs for HEATs [15]-[16]. In spite of this common trend, a higher-fidelity forward model that uses more detailed tractor model, battery model, and subsystem controller for diesel-generator set (GENSET), as well as mixed working cycles, has been constructed for validation purposes.

The main goal of this paper is modeling a series-type HEAT and designing two benchmark PMSs, i.e., a TC strategy and a PFC strategy, for the HEAT. The fuel economy and emissions in typical working cycles are evaluated for these two PMSs. Simulation studies are carried out to demonstrate the effectiveness of the HEAT model and control strategies. Compared with the TC strategy, the PFC strategy achieves better performance with regard to fuel economy and pollutant emissions. This work provides a foundation for the authors' future studies on the optimal power management and powertrain platform development for HEATs.

The rest of the paper is organized as follows. The system description and powertrain model are described in Section II. The two rule-based control strategies are introduced in Section III. Simulation results are provided and discussed in Section IV. Section V summarizes the paper.

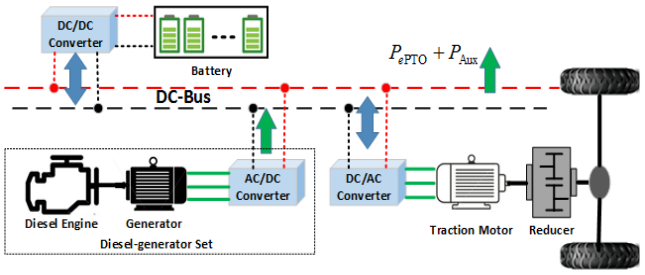

Fig. 1. Configuration of a series HEAT.

II. System Description and Modeling

A. System Configuration

As shown in Fig. 1, the series HEAT considered is mainly composed of four parts: 1) the prime source of energy consisting of a turbocharged diesel internal combustion engine and a permeant magnet synchronous generator, which is electrically connected to the DC-bus through an AC/DC converter; 2) a lithium-ion battery pack used as an energy buffer and controlled by a bidirectional DC-DC converter; 3) a permanent magnet synchronous motor providing the tractive force required by the wheels and the drawbar force demanded by the implement; and 4) the power take-off and power of auxiliaries drawn from the DC-bus for the combined tractor-implement electrification system.

For the purpose of assessment, a forward model is created mostly in MATLAB Simulink and Simscape. This dynamic model takes the inertia of the powertrain components into account. The supervisory controller is designed to distribute the power between the GENSET and the battery. A "driver model" based on an anti-windup PI controller is used to track the target duty cycle by controlling the acceleration and deceleration pedals.

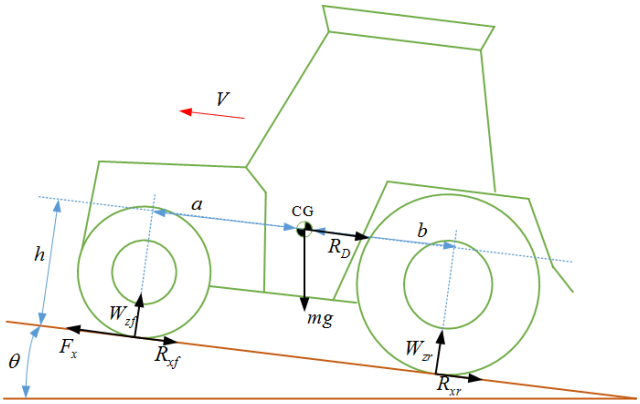

Fig. 2. Forces acting on an AT moving on an inclined field.

B. Tractor and Tire Models

Fig. 2 shows the forces acting on an AT moving on the ground with gradient. Since the AT features complex tire-terrain interaction, the dynamic axle loads and tire model are considered. The force equations of the tractor along the longitudinal axis can be expressed as [17]

$$\begin{aligned} m\dot{V} &= F_x - R_D - R_{roll} \\ R_D &= R_{aero} + R_{grad} + R_{draft} \\ &= 0.5\rho C_d A_F \left(V + V_{wind}\right) + mg\sin(\theta) + F_{draft} \\ R_{roll} &= R_{xf} + R_{xr} = C_r W_{zf} + C_r W_{zr} \\ W_{zf} &= \left[-h\left(R_D + m\dot{V}\right) + b\cdot mg\cos(\theta)\right]/(a+b) \\ W_{zr} &= \left[+h\left(R_D + m\dot{V}\right) + a\cdot mg\cos(\theta)\right]/(a+b) \end{aligned} \tag{1}$$

where F_x is the longitudinal traction force from driven wheels; R_D is the total drag force acting on the center of gravity (CG); R_{aero}, R_{roll}, R_{grad}, and R_{draft} are the aerodynamic, rolling resistance, gradient drag, and implement draft forces, respectively; W_{zf} and W_{zr} are the normal force acting on the front and rear tires; ρ is the mass density of air; C_d is the aerodynamic drag coefficient; A_F is the frontal area of the vehicle; V and V_{wind} are the tractor and wind velocities, respectively; C_r is the tire rolling resistance coefficient; m is the mass of the tractor; g is the acceleration due to the gravity; θ is the angle of field inclination; h is the height of CG above the ground; a and b are the distance from the front and rear axles to the CG, respectively.

A semi-empirical tire model widely used to calculate the steady-state tire force and the moment characteristics in vehicle dynamics studies is based on the so-called Magic Formula [18]. The model is capable of describing the basic tire characteristics for the intersection forces between the tire and the ground under several steady-state operating conditions. The Magic Formula is described as

$$F_x\left(\kappa, W_{zf}\right) = W_{zf} D \sin\left[C \arctan\left\{B\kappa - E\left(B\kappa - \arctan B\kappa\right)\right\}\right] \quad (2)$$

where κ is the tire slip ratio; B, C, D, and E are coefficients.

C. Engine and Electric Machine Models

Driven by the need for fast simulation time, some components such as engine and motors are typically simulated using "lookup maps." This approach is the most widely adopted methodology in the powertrain modeling of HEVs.

The fuel consumption rate of an engine can be modeled as a function of engine torque and speed, which is called the brake specific fuel consumption (BSFC) map.

$$BSFC = \frac{\dot{m}_f}{P_{Eng}} = \frac{f_{Eng}\left(T_{Eng}, \omega_{Eng}\right)}{T_{Eng} \cdot \omega_{Eng}} \quad (3)$$

The engine torque is formulated as

$$T_{Eng} = \alpha T_{WOT}\left(\omega_{Eng}\right) \quad (4)$$

where $\dot{m}_f$ is the engine fuel consumption rate, T_{Eng} is the engine torque, ω_{Eng} is the engine speed, α is the throttle opening angle, T_{WOT} is the wide-open-throttle (maximum) engine torque versus engine speed.

Non-road engines are an important source of air pollutants such as nitrogen oxides (NO_x), particulate matter (PM), and carbon monoxide (CO) [1]. Here, the lookup maps for these pollutants are adopted to compare the emissions.

The electric machines and inverter can also be modeled by means of efficiency maps where desired values of torque or speed are used as control inputs. The power consumed when motoring and recovered when regenerative braking can be expressed as

$$P_{EM} = \omega_{EM} \cdot T_{EM} \cdot \eta\left(\omega_{EM}, T_{EM}\right)^{\mathrm{sig}(-T_{EM})} \quad (5)$$

where ω_{EM}, T_{EM}, and η are the speed, torque, and efficiency of the electric machine, respectively; and sig(·) is a signum function.

By combining the diesel engine and generator efficiency data, a GENSET's optimal operating line (OOL) regarding fuel rate is obtained.

D. Battery Model

The Li-ion batteries are selected in this paper as they offer higher energy density and efficiency than other battery technologies [19]. This makes them more attractive for off-road vehicle applications.

The battery model is based on a modified Shepherd curve-fitting model, where an additional term (voltage polarization) is added to the battery discharge voltage expression to better present the effect of the battery SOC on the battery performance [20]. This model has been adopted by many papers for simulating Li-ion batteries [19]-[22]. The battery voltage in the discharge mode is given by

$$U_{bat}\left(it, i^*, i_{bat}\right) = U_0 - K\frac{Q}{Q - it}it - K\frac{Q}{Q - it}i^* - R_{bat}I_{bat} + A_e e^{-B_e \cdot it} \quad (6)$$

And the battery voltage in the charge model is

$$U_{bat}\left(it, i^*, i_{bat}\right) = U_0 - K\frac{Q}{Q - it}it - K\frac{Q}{it + 0.1Q}i^* - R_{bat}I_{bat} + A_e e^{-B_e \cdot it} \quad (7)$$

where U_{bat} is the nonlinear output voltage; U_0 is the constant voltage; K is the polarization constant; it is the extracted capacity; i^* is the low frequency current; I_{bat} is the battery current; Q is the maximum battery capacity; A_e is the exponential zone amplitude; B_e is the exponential zone time constant inverse; and R_{bat} is the battery internal resistance. These parameters can be extracted by the characterization of commercial batteries.

E. Load Model and Mixed Working Cycles

The load model consists of the tractor speed profile, draft force, and electrical PTO power for implements operation. In the simulation, the draft force is applied on the tractor by means of an ideal force source. The electrical power is simplified as designated currents drawn from the DC bus using programmable power sinks [22].

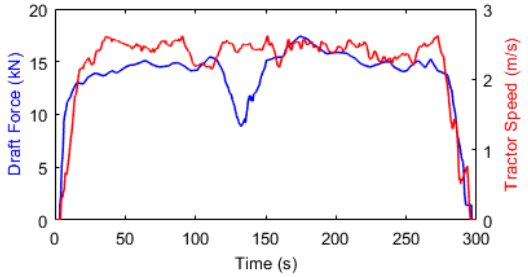

Fig. 3. Plough cycle for an agricultural tractor.

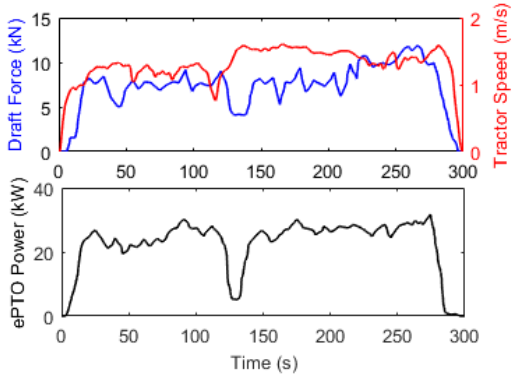

Fig. 4. Harvest cycle for an agricultural tractor.

Two mixed working cycles are designed to represent the typical plough and harvest operations. The Plough Cycle is characterized by heavy tractive work as shown in Fig. 3. The Harvest Cycle features medium tractive work and heavy electrical power demand as illustrated in Fig. 4.

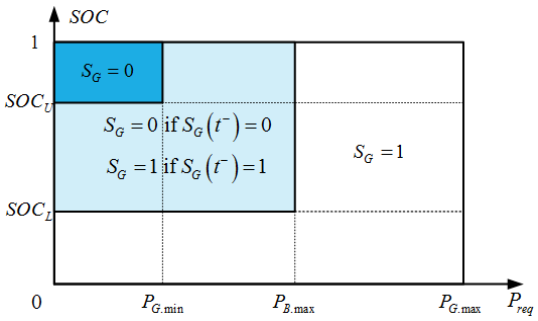

Fig. 5. Engine on/off map when using the PF strategy.

III. Rule-Based Power Management Strategy

The control strategy for a series HEAT is straightforward, running the GENSET at its most fuel efficiency points or along the OOL by controlling the throttle position and generator torque. The GENSET will be turned off when the predefined conditions are satisfied. In this work, two traditional rule-based control strategies are investigated.

A. Thermostat Control Strategy

The TC is a rule-based on/off strategy and runs the engine at its optimal operating point (OOP). The GENSET will be turned off (S_G = 0) when the SOC reaches its upper threshold SOC_U and turned on (S_G = 1) when the SOC approaches its lower threshold SOC_L. The corresponding power distribution can be defined as

$$P_G(t) = \begin{cases} 0 & \text{if } S_G = 0 \\ P_{OOP} & \text{if } S_G = 1 \end{cases} \tag{8}$$

$$P_B(t) = \begin{cases} 0 & \text{if } SOC(t) < SOC_L \\ P_{req}(t) - P_G(t) & \text{if } SOC_L \le SOC(t) \le SOC_U \\ P_{req}(t) & \text{if } SOC(t) > SOC_U \end{cases} \tag{9}$$

where P_G, P_B, P_{OOP}, and P_{req} are the GENSET output power, the battery power, the GENSET power at the OOP, and the required power.

B. Power Follower Control Strategy

For the PFC strategy, the GENSET is designated as the primary power source to meet the power demand under almost all working conditions, in addition to the cases when the required power is low and the SOC is greater than the upper SOC limit. The control logic of the GENSET is shown in Fig. 5 and the output power is determined by the following:

$$P_G(t) = \begin{cases} P_{G.\min} & \text{if } SOC(t) \ge SOC_U \\ P_m(t) & \text{if } \mathrm{SOC}_L < SOC(t) < SOC_U \\ P_{G.\max} & \text{if } SOC(t) \le SOC_L \end{cases} \tag{10}$$

$$P_m(t) = P_{req}(t) + P_{ch}\left[\frac{SOC_U + SOC_L}{2} - SOC(t)\right] \tag{11}$$

$$P_B = \begin{cases} P_{req} & \text{if } S_G = 0 \\ P_{req} - P_G & \text{if } S_G = 1 \end{cases} \tag{12}$$

Due to the reduction of the battery usage, the PFC can extend the battery life and decrease the power losses during charging and discharging.

IV. Simulation Results and Discussions

The two rule-based PMSs are tested on the series HEAT model to investigate the operation and performance with different working cycles. For all the simulations, the initial SOC is 51%, and the SOC's upper and lower thresholds are 70% and 50%, respectively.

A. Basic Characteristics

Firstly, the characteristics of the two PMSs are compared with one Plough Cycle. It can be seen from Fig. 6 that the tractor can track the reference speed of the cycle well. Since the TC just uses a single OOP, the GENSET provides a constant power after the GENSET starts, as shown in Fig. 7, and its operating points converge to the OOP which is depicted in Fig. 8. However, the GENSET delivers changeable power as presented in Fig. 9, and the operating points of the PFC moves along the OOL in Fig. 10.

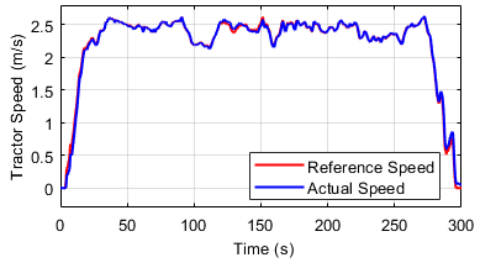

Fig. 6. Speed profiles of the tractor for Plough Cycle.

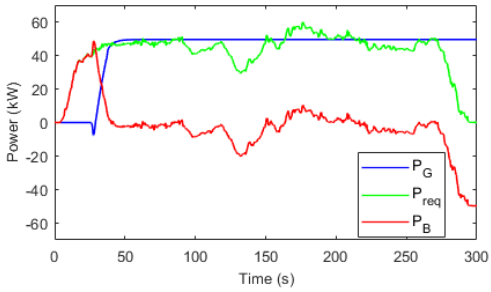

Fig. 7. Power profiles for Plough Cycle with the TC strategy.

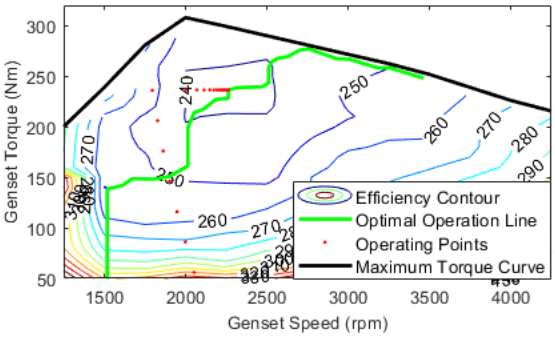

Fig. 8. GENSET operating points for Plough Cycle with the TC strategy.

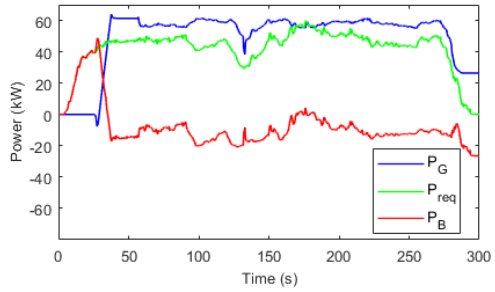

Fig. 9. Power profiles for Plough Cycle with the PFC strategy.

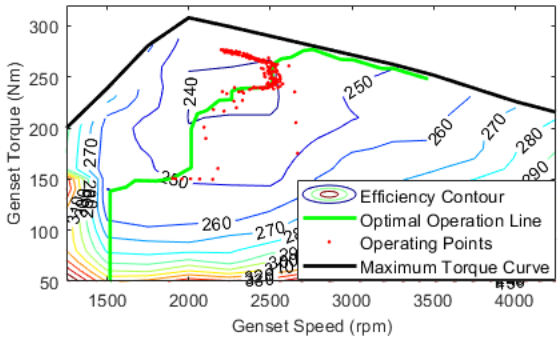

Fig. 10. GENSET operating points for Plough Cycle with the PFC strategy.

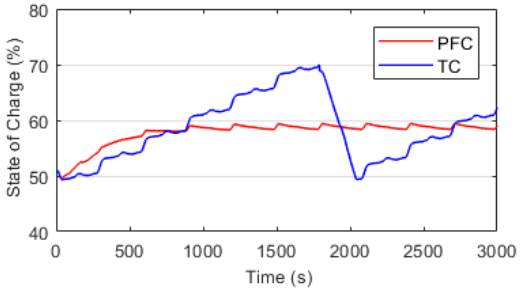

Fig. 11. SOC profiles of two control strategies for ten Plough Cycles.

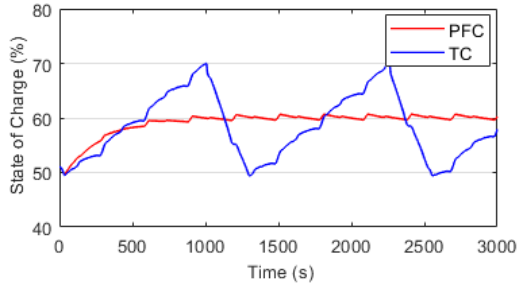

Fig. 12. SOC profiles of two control strategies for ten Havester Cycles.

B. State of Charge Profiles

Secondly, repeated working cycles are used to study the SOC profiles. Figs. 11 and 12 show the SOC curves corresponding to ten Plough Cycles and ten Harvester Cycles, respectively. It is clear that the battery is discharged and charged alternately when the TC strategy is used. When the SOC approaches the upper boundary, the GENSET is off, and the SOC is depleted quickly. On the contrary, when the PFC is used, the SOC is almost sustained when the SOC oscillates at 60%. The battery seldom provides the required power alone. It is worth noting that the charging and discharging in the case of TC is much more aggressive than that in the case of PFC. Accordingly, the battery suffers from heavier burden and larger resistive losses.

C. Fuel Economy and Emissions

To fairly compare the fuel economy, equivalent fuel consumption (EFC) is usually used by incorporating the *equivalent factor* between electrical and chemical energy consumption [23]. The EFC can be described as

$$EFC = m_f + s(t)\cdot \Delta SOC \cdot \frac{Q_B \cdot V_{B,OC}}{Q_{LHV}} \tag{13}$$

where m_f is the fuel consumption of the engine; s is the equivalent factor; Q_B is the battery capacity; $V_{B,OC}$ is the battery open-circuit voltage; Q_{LHV} is the fuel lower heating value; ΔSOC is the SOC difference between the initial and final conditions.

Simulation results for the fuel economy and emissions are summarized in Table I. Although the GENSET in the case of TC works at the most efficient point, the total fuel consumption and EFC is larger than that in the case of PFC for the same working cycle. The main reason is that the resistive losses in the battery and DC/DC converter are very large when the battery is charged and discharged with a large current. Therefore, the efficiency of the entire powertrain drops significantly. It can be seen that the CO and NO_x production in the case of PFC is also less than that in the case of TC, but the PFC produces more PM emissions. This is because the operating points of the GENSET are optimal for fuel consumption rather than emission. In addition, the state transitions of the GENSET between OFF and ON are accompanied by considerable fuel and emission costs.

TABLE I. FUEL CONSUMPTION AND EMISSION COMPARISONS

	Plough Cycle × 10		**Harvester Cycle × 10**	
	TC	***PFC***	***TC***	***PFC***
Fuel [kg]	10.004	9.659	8.890	8.617
SOC [%]	62.324	59.998	57.879	60.261
EFC [kg]	9.799	9.496	8.765	8.450
CO [g]	33.836	32.058	35.115	28.302
PM [g]	4.498	5.442	3.973	5.679
NO_x [g]	240.758	225.397	214.493	193.897

V. CONCLUSIONS

In this paper, a series-type HEAT was modeled with a high fidelity of tractor dynamics and energy sources. The power management of the HEATs is required to take the mixed power loads and various working patterns into consideration. Two benchmark PMSs, namely, TC and PFC, were studied with the HEAT model. The tractor performance regarding fuel economy and emissions for different operation cycles were compared by simulations. The results presented that the PFC is capable of saving fuels and reducing NOx and CO emissions. Moreover, the PFC relieved the stress of

battery and improved the overall efficiency of the powertrain system. However, one drawback of the PFC is that it produces more PM. Thus, further investigation is required to distribute the power of the HEAT in an optimal way to improve the performance in both fuel economy and emissions.

REFERENCES

[1] T. Dallmann and A. Menon, "White paper: Technology pathways for deisel engines used in non-road vehicles and equipment," *The Internationl Council on Clean Transportation*, Sept. 2016.

[2] C. Monnay, "Benchmark survey: potential and trends in off-high way vehicles' electrification," *Semcon*, Aug., 2017. [Online]. Available: https://semcon.com/main-offers/electrification/potentia-and-trends-in-off-highway-vehicles-electrification/

[3] A. Munoz-Garcia and P. Barreiro, "High voltage electrification and agricultural machinery–A review," *Energy Convers and Maneg.t*, vol. 115, pp. 117-131, 2016.

[4] E. A. Burning, "Electri drives in agricultural machinery – Approach form the tractor side," *Journal of Agicultural Engineering*, vol. 47, pp. 30-35, 2010.

[5] N. Jalil, A. Kheir, and M. Salman, "A rule-based energy management strategy for a series hybrid vehicle," in *Proc. Amer. Control Conf*., pp. 689-693, 1997.

[6] S. G. Li., F. C. Walsh, and C. N. Zhang, "Energy and battery management of a plug-in series hybrid electric vehicle using fuzzy logic," *IEEE Trans. Vel. Technol.*, vol. 60, no. 8, pp. 3571–3585, Oct. 2011.

[7] F. R. Salmasi, "Control strategies for hybrid electric vehicle: evolution, classification, comparison, and future trends," *IEEE Trans. Control Syst. Technol*., vol. 56, no. 5, pp. 2393-2404, May 2007.

[8] M. Kim, D. Jung, and K. Min, "Hybrid thermostat strategy for enhaning fuel economy of series hybrid intracity bus," *IEEE Trans. Vel. Technol.*, vol. 63, no. 8, pp. 3569–3579, Oct. 2014.

[9] W. Shabbir and S. A. Evanglou, " Exclusive operation strategy for the supervisory control of series hybrid electric vehicles," *IEEE Trans. Control Syst. Technol.,* vol. 24, no. 6, pp. 2190-2198, Nov. 2016.

[10] Y. Ko, J. Lee, and H. Lee, "A supervisory control algorithm for a series hybrid vehicle with multiple energy source," *IEEE Trans. Vel. Technol.*, vol.64, no. 11, pp. 4942–4953, Nov. 2015.

[11] J. Gao, F. Sun, H. He, G. G. Zhu, and E. G. Strangas, "A comparative study of supervisory control strategies for a series hybrid electric vehicle," in *Proc. Asia-pacific Power Energy Eng. Conf. (APPEEC)*. pp. 1-7, Mar. 2009.

[12] L. Xu, J. Zhang, M. Liu, Z. Zhou, and C. Liu, "Control algorithm and energy management stategy for extended range electric tractors," *Int. J. Agric. & Biol. Eng.*, vol. 10, no. 5, pp. 35-44, Sept. 2017.

[13] *Definitions and Classifications of Agricultural Field Equipment*, American Society of Agricultural and Biological Engineers (ASABE) Standards. S390.5, Jan. 2011.

[14] O. Noren and O. Pettersson, "Development of relevant work-cycles and emission factors for off-road machines," *SAE Technocal Paper* 2001-01-3637. Sept. 2001.

[15] H. Mousazadeh, A. Keyhani, and A. Javadi, "Optimal power and energy modeling and range evaluation of a solar assist plug-in hybrid electric tractor (SAPHT)," *Transactions of the American Society of Agricultural and Biological Engineers*, vol. 54, no. 4, pp. 1025-1035, 2010.

[16] H. Yi, J. Kim, Y. park, and S. Cha, "Fuel saving of power train modeling in the parallel hybrid tractor," in *Proc. EVS28 International Electric vehicle Symposium and Exhibition*, May 2015.

[17] R. Rajamani, *Vehicle Dynamics and Control, 2nd ed.*, New York: Springer, 2012.

[18] H. B. Pacejka and I. Besselink, *Tire and Vehicle Dynamics, 3rd ed*., Amsterdam, Netherlands: Elsevier, 2012.

[19] P. Garcia, J. P. Torreglosa, L. M. Fermandez, and F. Jurado, "Viability study of a FC-battery-SC tramway controlled by equivalent consumtion minimization strategy," *Int. J. Hydrogen Energy*, vol. 37, no. 11, pp. 9368-9382, Jun. 2012.

[20] O. Tremblay, L.-A. Dessaint, and A.-I Dekkiche, "A generic battery model for the dynamic simulation of hybrid electric vehicles," in *Proc. IEEE Vehicle Power and Propulsion Conference*, pp. 284-289, Sept. 2007.

[21] S. N. Motapon, L. A. Dessaint, and K. Al-Haddad, "A comparative study of energy management schemesfor a fuel-cell hybrid emergency power system of more-electric aircraft," *IEEE Trans. Ind. Electron.*, vol. 61, no. 3, pp. 1320-1334, Mar. 2014.

[22] Y. Kim, V. Raghunathan and A. Raghunathan, "Design and management of battery-suercapacitor hybrid electrical energy storage systems for regualtion services*," IEEE Trans. Multi-scale Comput. Sys*., vol. 3, no. 1, pp. 12-24, Jan.-Mar., 2017.

[23] A. Sciarretta, M. back, and L. Guzzella, "Optimal control of parallel hybrid electric vehicles," *IEEE Trans. Control Syst. Technol.*,vol. 12, no. 3, pp. 352-363, May 2004